24th COBEM - 2017

24[th] ABCM International Congress of Mechanical Engineering
December 3-8, 2017, Curitiba, PR, Brazil

COBEM-2017-0173
ACTIVE VIBRATION CONTROL OF A FLEXIBLE STRUCTURE BY USING GENERALIZED PREDICTIVE CONTROL

Erik Taketa
Daniel Almeida Colombo
Edson Hideki Koroishi
Fabian Andres Lara-Molina
Departament of Mechanical Engineering, Federal University of Technology - Paraná, - Av. Alberto Carazzai n^o 1640 CEP 86300-000, Cornélio Procópio-PR, Brazil
eriktaketa@alunos.utfpr.edu.br, danielcolombo@alunos.utfpr.edu.br, edsonh@utfpr.edu.br, fabianmolina@utfpr.edu.br

Abstract. *Recently, the Active Vibration Control (AVC) has received great attention from researchers due to high potential for industrial applications. Additionally, the predictive control has made a significant impact on industrial control engineering. Thus, the present contribution addresses a study of the AVC of a mechanical system with one degree of freedom (1 -DOF) using the Generalized Predictive Control (GPC) by evaluating the dynamic performance with the aids of dynamic simulation. In order to analyze the results, the GPC responses are compared with a Linear Quadratic Regulator (LQR) responses. The results demonstrate the efficiency of GPC control methodology.*

Keywords: *Active Vibration Control, Generalized Predictive Control, Mass-Spring-Damper system*

1. INTRODUCTION

The vibrations that occur in machines, aircraft, structures and dynamic systems are undesirable because of the resulting unpleasant motions and the dynamic stresses which may lead to fatigue and failure of the structure or machine and also due to the reduction in performance which is associated with the vibrations.

In an industrial environment, there are several sources of vibration, such as impact processes, rotating or alternate machines, transport vehicles, fluid flow, and many others. The presence of vibration can often cause excessive wear of bearings, cracking or loosening of latches, and structural and mechanical failure. Occupational exposure of people to mechanical vibration can cause pain, discomfort, and reduce work efficiency.

The vibrations can be eliminated by using dynamic analysis of the structure, however, the manufacturing costs involved in vibration attenuation may be too high and infeasible for a particular design. The vibration control design must consider both the acceptable amount of vibration and the reasonable manufacturing cost. In some cases, the excitation force is inherent in the structure. Thus, even a relatively small excitation force may cause an undesirable near-resonance response, especially in slightly damped systems. Because of this, the application of vibration control in flexible structures becomes necessary (Rao and Yap, 2011) (Inman, 2006) (Ogata, 2010).

The control engineering has played a vital role in the advancement of science and engineering, thus becoming an important and integral part of modern industrial processes. The control of dynamic systems shows its importance due to the fact that all systems can receive disturbances that affect the output of the system, and thus, withdrawn from their normal behavior, either through noise or undesirable vibrations. Because of this, vibration control is considered a highly relevant technological challenge. Faced with this challenge, one of the ways to solve this problem is to use vibration control techniques, which can be divided into two main classes: passive and active. In addition to passive and active control techniques, we can also mention the semi-active and hybrid vibration control.

The techniques of passive control consist of modifying the dynamic characteristics of the system such as mass, stiffness, and damping in order to reduce vibrations and increase the stability of the same. The active control techniques deal with an efficient way to modify the dynamic characteristics of the system, aiming at the vibration attenuation and the ease of adaptation to environmental or operational changes. The semi-active and hybrid control uses the control in a way that combines the properties and advantages of passive and active controls (Koroishi et al., 2015) (Ogata, 2010).

Thus, the active vibration control (AVC) of flexible structures has been covered by a large number of excellent research papers due to its high potential for industrial applications (Koroishi et al., 2015) (Horst and Wölfel, 2004) (Mahfoud and Hagopian, 2010).

On the other hand, we have Predictive Control, or as also is know Model-Based Predictive Control (MPC), is one of the modern control techniques that originated in the later years Has developed considerably since then. The term Predictive

Control does not designate a specific control strategy, but a wide range of control methods that make explicit use of a process model to obtain control while minimizing performance criteria. Lately, these methods have become one of the modern control techniques that have a great impact on the control of industrial processes.

One of the most widespread predictive controllers in the literature is the Generalized Predictive Controller (GPC). These controllers are characterized by using predictions of the future behavior of the controlled system to perform the calculation of the optimal control law (Camacho and Alba, 2013) (Maciejowski, 2002) (Lara-Molina et al., 2014). Thus, in the present contribution, the aim is to design an active vibration control system through actuators using GPC. The study is carried out in a flexible structure of one degree of freedom (1 -DOF). For comparison purposes, the Linear Quadratic Regulator (LQR) controller is used. This numerical study illustrates the GPC analysis to evaluate how this control affects the performance of the structure. This type of control has the characteristic of calculating a sequence of future control actions in order to minimize a multi-step objective function defined under a prediction horizon. For this structural vibration control, we must first perform the system modeling, design the control scheme, tune the controller, and finally apply the control to the structure.

The remainder of this paper is organized into four sections. In section 2 we introduce the mathematical model of the system that will be used throughout this paper. Details of controllers LQR and GPC are described in this section. The results and discussion are presented in section 3, and further conclusions are given in sections 4.

2. MATERIALS AND METHODS

In this section the system modeling is presented, the control techniques used for the development of this paper are described. The following is the application of the case study is presented.

2.1 Modeling of mechanical structure

The mechanical systems the first step in order to study and analyze the dynamic performance of the controller within the structure. The physical models are simplified and abstract representations that describe the behavior of the systems of interest. Depending on the system considered and the particular circumstances involved, the mathematical models may take different forms, one mathematical model may be more appropriate than others. First, the constitutive relations, which characterize the behavior of the elements of the system are defined analytically or experimentally. Finally, the compatibility and continuity relations are introduced in order to have the complete system model (Norton, 2010) (Ogata, 2010) (Dorf and Bishop, 2009).

Once the mathematical model of a system is obtained, the computational or analytical tools can be used to obtain the analysis of the real system (Ogata, 2010).

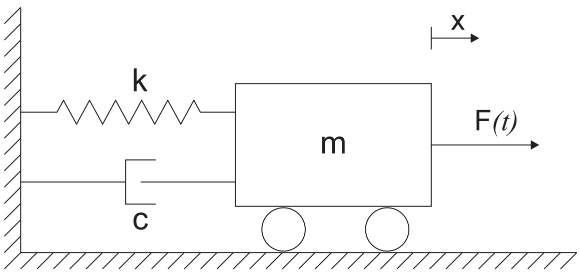

Figure 1. Mass-Stiffness-Damper Structure (1-DOF)

Thus, we obtain the equation of the motion of this structure using the Newton's second law.

$$m\ddot{x}(t) + c\dot{x}(t) + kx(t) = F(t) \tag{1}$$

Where m is the mass, c is the viscous damping, k is the stiffness, x is the displacement and F is the excitation force. Applying the Laplace transform to the motion equation of system (Eq. (1)). Considering zero initial conditions, we obtain:

$$ms^2X(s) + csX(s) + kX(s) = F(s) \tag{2}$$

Which can be organized as a relation between the output and the input.

$$H(s) = \frac{X(s)}{F(s)} = \frac{1}{ms^2 + cs + k} = \frac{1/m}{s^2 + 2\xi\omega_n s + \omega_n^2} \tag{3}$$

The $H(s)$ function is known as the transfer function of the system. Where the natural frequency is given by $\omega_n = \sqrt{k/m}$ and the damping factor $\xi = c/(2m\omega_n)$.

2.2 Generalized Predictive Control

The strategies of predictive control based on model differ among them, mainly in the model of the plant used and the functions of cost to be minimized. The main methods based on predictive control are: functional predictive control Richalet et al. and generalized predictive control Clarke et al.. In this work we will use generalized predictive control, a more detailed study can be found in (Clarke et al., 1987). The control law is obtained by minimizing a quadratic cost function as shown in the Fig. 2.

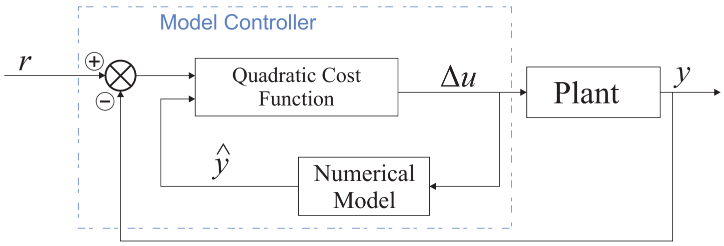

Figure 2. Control Scheme.

Fundamentally, the law of predictive control consists of an algorithm that calculates a future control sequence Δu. The main elements of the predictive controller are the numerical model of the plant to calculate the predictive output $\hat{y}$ and the quadratic cost function to minimize future error: $r - \hat{y}$ in a finite prediction horizon h. The basic steps of model-based predictive control are summarized as follows:

1. Definition of a numerical model of the plant to predict future output $\hat{y}$.
2. Minimizing a quadratic cost function over a finite prediction horizon h using the prediction of error $r - \hat{y}$. For this, the trajectory has to be defined in the future time.
3. From the minimization of the cost function, obtaining an optimal sequence of increments in the control Δu in the finite prediction horizon h.
4. Only the first element of the optimal control sequence Δu is applied to the plant, the other elements of this sequence being neglected.
5. Iteration of the previous procedure in the next sampling period to recalculate the increment of the optimal sequence Δu, in accordance with the control strategy based on the receding horizon control strategy.

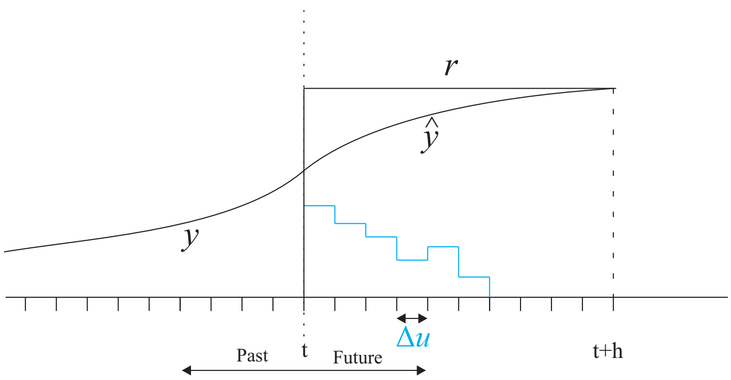

Figure 3. Receding Prediction Horizon.

The following are the principles and a brief description of the generalized predictive control formulation. In linear GPC theory, the plant is modeled using the CARIMA model:

$$A(z^{-1})y(t) = B(z^{-1})u(t-1) + \frac{C(z^{-1})\xi(t)}{\Delta(z^{-1})} \tag{4}$$

With $u(t)$, $y(t)$ the input and output of the plant, $\xi(t)$ centered Gaussian white noise, and $C(z^{-1})$ model the influence of noise. The difference operator $\Delta(z^{-1}) = 1 - z^{-1}$ helps eliminate static noise by introducing integrative action into the model. The control is obtained by minimizing the quadratic cost function J given by:

$$J = \sum_{j=N_1}^{N_2} [r(t+j) - \hat{y}(t+j)]^2 + \lambda \sum_{j=1}^{N_u} \Delta u(t+j-1)^2 \tag{5}$$

Where, N_1 and N_2 define the beginning and end of the prediction horizon of the output, and N_u defines the control horizon. Λ is the weighting factor, $r(t)$ is the reference, $\hat{y}(t)$ is the output obtained by solving the Diophantine equation, and $u(t)$ is the control. The "receding horizon" principle states that only the first value of the resulting optimal control sequence $\Delta u(t)$ from the minimization of the quadratic cost function $(\delta J/\delta \Delta u)$ of the Eq. (5) is applied to the system. For the sampling period, the following process is repeated.

The controller design consists of adjusting the parameters: N_1, N_2, N_u, and λ to satisfy input and output behavior while retaining stability requirements (Boucher and Dumur, 1996). With this control strategy, the controller is obtained in the RST form.

2.3 Linear Quadratic Regulator

The optimal control theory, especially that of the linear quadratic regulator (LQR), consists in the assumption of adopting a performance index through which it is possible to optimize physical quantities. According to Ogata, the problem of the quadratic linear regulator allows to determine the matrix $[G]$ of the optimal control vector given by the Eq. (6) in order to minimize the performance index given by Eq. (7).

$$u(t) = -[G]x(t) \tag{6}$$

$$J = \int_0^\infty \left(\{x(t)\}^T [Q_{lqr}] \{x(t)\} + \{u(t)\}^T [R_{lqr}] \{u(t)\} \right) dt \tag{7}$$

In which, $[Q_{lqr}]$ is a Hermitian matrix symmetric positive or semi-definite positive or real symmetric and $[R_{lqr}]$ is a Hermitian matrix symmetric positive or real defined. Ogata highlights that the second term on the right-hand side of the Eq. (7) represents the power consumption of the control signals. Substituting the Eq. (6) into the Eq. (7) and making the necessary simplifications, obtains:

$$J = \int_0^\infty \left(\{x(t)\}^T \left([Q_{lqr}] + [G]^T [R_{lqr}][G] \right) \{x(t)\} \right) dt \tag{8}$$

By minimize the J performance index leads to the follow expression:

$$\{x(t)\}^T \left([Q_{lqr}] + [G]^T [R_{lqr}][G] \right) \{x(t)\} = -\frac{d(\{x(t)\}^T [P_{lqr}] \{x(t)\})}{dx} \tag{9}$$

Ogata shows that the gain matrix $[G]$ is given by the Eq. (10).

$$[G] = [T_{lqr}]^{-1} ([T_{lqr}]^T)^{-1} [B]^T [P_{lqr}] \tag{10}$$

In which the matrix $[T_{lqr}]$ is the singular matrix given by:

$$[R_{lqr}] = [T_{lqr}]^T [T_{lqr}] \tag{11}$$

The matrix $[P_{lqr}]$ is obtained by solving the Riccati matrix equation given by Eq. (12).

$$[A]^T[P_{lqr}]+[P_{lqr}][A]-[P_{lqr}][B][R_{lqr}]^{-1}[B]^T[P_{lqr}]+[Q_{lqr}]=0 \quad (12)$$

Substituting the matrix $[P_{lqr}]$ obtained in the Eq. (12) in the Eq. (10), we determine the value of the gain matrix $[G]$, which is given in the following form:

$$[G]=R_{lqr}^{-2}(B^TP_{lqr}+T_{lqr}^T) \quad (13)$$

2.4 Case Study Application

The system studied is approximated as a mass-spring-damper system, this structure is composed of an aluminum platform supported by 4 stainless steel beams and two electromagnetic actuators of opposite sides, as show in Fig. 4-a. In order to obtain the model of 1-DOF presents in Fig. 4-b, it is realized through the equation of motion of this structure, where, m, k and c are mass, stiffness and damping, respectively.

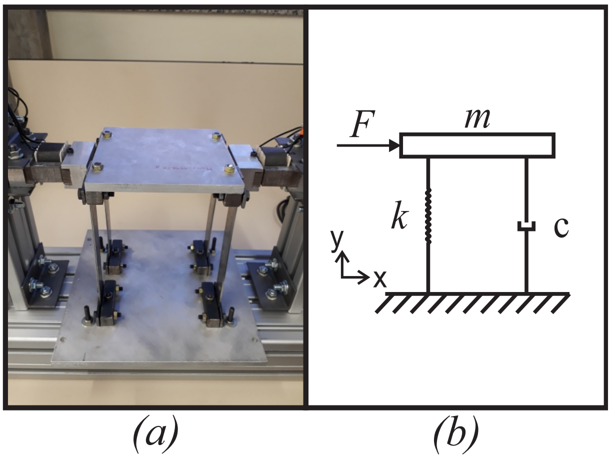

Figure 4. Mass-Stiffness-Damper Structure

To perform the procedure of analysis of the mechanical system of one degree of freedom, the parameters were identified. Thus, once the parameters of the mechanical system were obtained, these parameters were applied to the model. With the system modeled and with its parameters entered, the tuning of the LQR and GPC controllers is performed. Once the controllers are tuned, the control is applied to the structure and analyzed the results to verify the performance of each controller.

The mechanical structure is subjected to an initial displacement of 0.05 m. For tuning of the mass-spring-damper system controller, the previously obtained parameters are used, through the identification, stiffness $k = 6777.4\ N/m$ and damping $c = 8.0559\ N.s/m$. The mass parameter $m = 1.5962\ Kg$, was obtained using a precision balance. With the defined parameters, the controller LQR and GPC are tuned to the mass-spring-damper structure.

2.4.1 Tuning LQR Controller

The controller has been tuned to get a response with a small damping. For the tuning of the LQR controller was performed through the trial and error method. Where it reached the values of:

$$Q=\begin{bmatrix}10 & 0\\ 0 & 10\end{bmatrix} \quad (14)$$

$$R=0.025 \quad (15)$$

Solving the riccati equation, presented in the Eq. (12), we obtain the value of P_{lqr}.

$$P_{lqr}=\begin{bmatrix}228.8704 & 0.0001\\ 0.0001 & 0.0539\end{bmatrix} \quad (16)$$

The gain obtained from the LQR controller was:

$$K_{lqr} = \begin{bmatrix} 0.0148 & 8.2212 \end{bmatrix} \tag{17}$$

2.4.2 Tuning GPC Controller

For tuning the GPC controller parameters, N_1, N_2, N_u e λ Successive attempts were made to choose the best gains, thus obtained the following parameters: $N_1 = 1, N_2 = 40, N_u = 1$ e $\lambda = 6.38 \times 10^{-6}$. Thus, obtaining the following values for the RST polynomials:

- $R = 3.8190e4 - 7.5338e4z^{-1}3.7838e4z^{-2}$
- $S = 1.0000 - 0.9257z^{-1} - 0.0743z^{-2}$
- $T = 4.6170 + 4.2549z^{-1} + 4.2954z^{-2} + 4.7425z^{-3} + 5.5895z^{-4} + 6.8188z^{-5} + 8.4027z^{-6} + 10.3033z^{-7} + 12.4741z^{-8} + 14.8606z^{-9} + 17.4020z^{-10} + 20.0326z^{-11} + 22.6833z^{-12} + 25.2838z^{-13} + 27.7642z^{-14} + 30.0568z^{-15} + 32.0982z^{-16} + 33.8308z^{-17} + 35.2045z^{-18} + 36.1781z^{-19} + 36.7206z^{-20} + 36.8122z^{-21} + 36.4445z^{-22} + 35.6216z^{-23} + 34.3597z^{-24} + 32.6867z^{-25} + 30.6421z^{-26} + 28.2756z^{-27} + 25.6462z^{-28} + 22.8205z^{-29} + 19.8715z^{-30} + 16.8761z^{-31} + 13.9135z^{-32} + 11.0632z^{-33} + 8.4024z^{-34} + 6.0045z^{-35} + 3.9368z^{-36} + 2.2584z^{-37} + 1.0192z^{-38} + 0.2576z^{-39} + 0z^{-40}$

In this way, we have the following frequency characteristics of the stable corrected system:

- Gain Margin = 22.89 dB
- Phase Margin = 84.53^o
- Delay Margin = $16.80 \times T_e$

The closed-loop system stability using the GPC controller is ensured through the following criteria:
In the Figure 5 it is observed that the closed-loop poles are inside the unit circle.

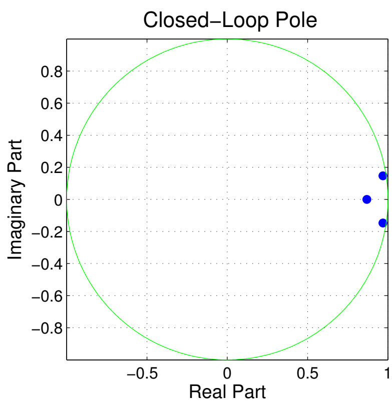

Figure 5. Closed-Loop Pole

In the Figure 6 it is seen that the gain margin = 22.89 dB, and the phase margin = 84.53^o.

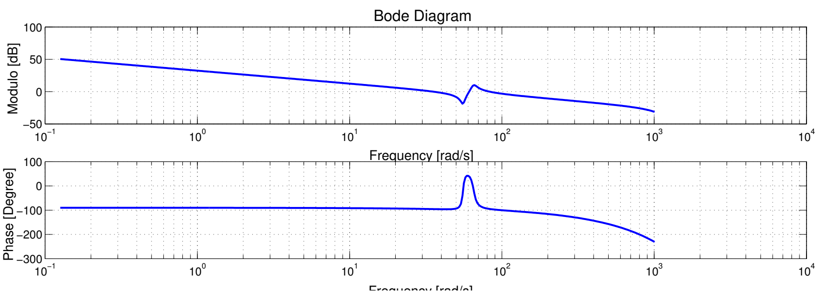

Figure 6. Bode Diagram

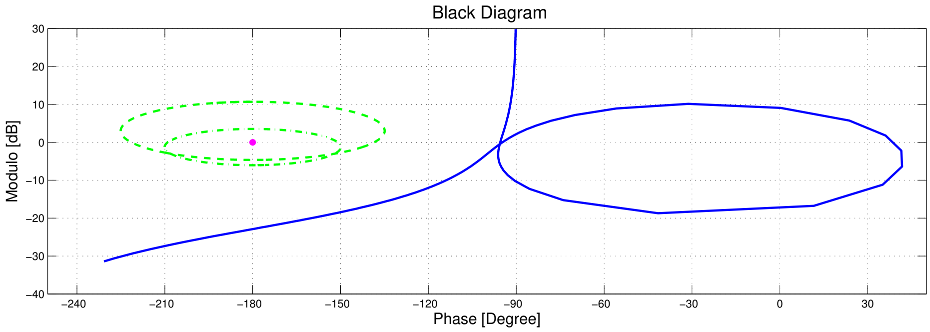

Figure 7. Closed-Loop Black Diagram

In Figure 7 it is verified that the frequency curve is outside the area defined by the iso-gain curves, in this way at least a phase margin and a gain margin is assured.

With the obtained model and the tuned controllers, the GPC and LQR controls are applied in the structure for comparison.

3. RESULTS AND DISCUSSIONS

The study is performed through numerical simulations of a 1 degree freedom system and the free natural frequency obtained is $9,985$ HZ as shown in the Fig.8. In the same figure we can see the FRF using LQR and GPC.

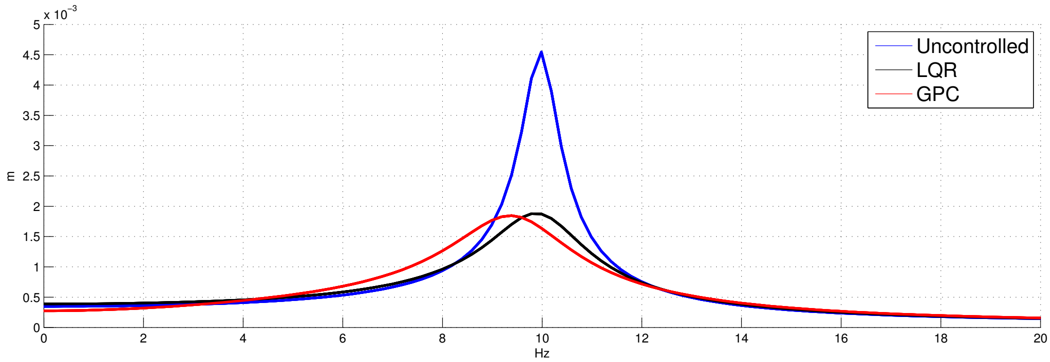

Figure 8. Frequency Response

In the Figure 9, its possible observe the behavior of the mechanical system for an initial displacement of 0.05 m. In the first series of data, blue color, represents the system without control, the data described in black represents the behavior of the system with the LQR control, finally, the series of data in red presents the behavior of the system using the GPC. The dashed lines represent 5% of the maximum system displacement. Note that the GPC control remains in the 5% regime before the LQR control.

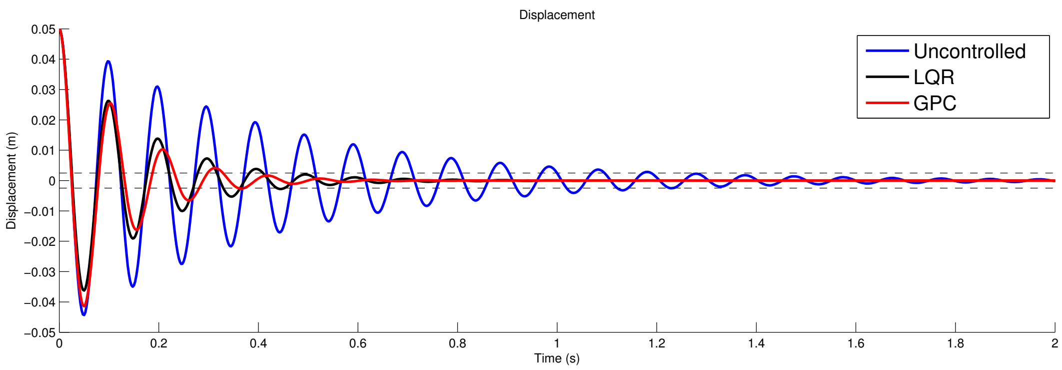

Figure 9. Displacement

The results of the Fig. 9 indicates that the controller obtained by GPC method is capable of stabilizing better than LQR. The GPC control enters the range of 5% in 0.3825 seconds while the LQR in 0.4625 seconds.

In the Fig. 10, the control forces of the controllers are shown in the unit of force Newton (N). The graphic demonstrates the control forces of LQR (black) and GPC (red), dashed lines representing 5% of the maximum force applied to the system. The GPC control remains in the 5% regime before the LQR, but the control force in the initial moments are higher than LQR.

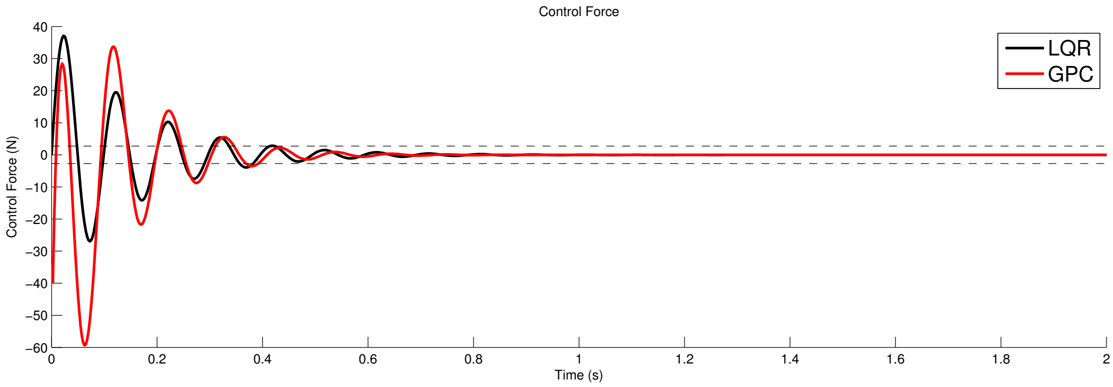

Figure 10. Control Force

The control force in Fig. 10 the amplitude of GPC method was 59.02% higher than LQR. However, the GPC control enters the range of 5% in 0.3925 seconds while the LQR in 0.4225 seconds.

4. CONCLUSIONS

This work presented the project and implementation of GPC controller in the 1-DOF mass-damping-stiffness structure. While the predictive control has been receiving an increase in the interest of researches, it is possible to perceive the difficulties for the control in real time. Despite these difficulties, the GPC when compared to the LQR demonstrated to meet the expectations.

Summarizing, the simulation results obtained attained the performance specifications imposed on the system, which shows that the projected GPC controller was satisfactory for the active vibration control of studied system.

Additionally, in future works, we will add parametric uncertainties in the system to verify the robustness of the GPC controller.

5. ACKNOWLEDGMENTS

This work was done with support of CAPES, Coordenação de Aperfeiçoamento de Pessoal de Nível Superior, and Universidade Tecnológica Federal do Paraná (UTFPR) - Campus Cornélio Procópio.

6. REFERENCES

Rao, S. S.; Yap, F. F. *Mechanical vibrations*; Prentice Hall Upper Saddle River, 2011; Vol. 4.
Inman, D. J. *Vibration with Control*, first edition ed.; Jhon Wiley and Sons: New York - NY, 2006.
Ogata, K. *Engenharia de Controle Moderno*, fifth edition ed.; Pearson Prentice Hall: São Paulo-SP, Brazil, 2010.
Koroishi, E. H.; Molina, F. A. L.; Faria, A. W.; Steffen Junior, V. *Journal of Aerospace Technology and Management* **2015**, *7*, 70–80.
Koroishi, E.; Faria, A.; Lara-Molina, F.; Steffen Jr, V. Fuzzy Modal Control Applied to Smart Composite Structure. Journal of Physics: Conference Series. 2015; p 012090.
Horst, H.-G.; Wölfel, H. *Journal of Intelligent Material Systems and Structures* **2004**, *15*, 721–728.
Mahfoud, J.; Hagopian, J. D. *Journal of Aerospace Engineering* **2010**, *24*, 329–337.
Camacho, E. F.; Alba, C. B. *Model predictive control*; Springer Science & Business Media, 2013.
Maciejowski, J. M. *Predictive control: with constraints*; Pearson education, 2002.
Lara-Molina, F. A.; Maurício Rosário, J.; Dumur, D.; Wenger, P. *Industrial Robot: An International Journal* **2014**, *41*, 275–285.
Norton, R. L. *Cinemática e dinâmica dos mecanismos*; AMGH Editora, 2010.
Dorf, R. C.; Bishop, R. H. *Edição, Editora LTC* **2009**,
Richalet, J.; el Ata-Doss, S. A.; Arber, C.; Kuntze, H.; Jacubasch, A.; Schill, W. *IFAC Proceedings Volumes* **1987**, *20*,

251–258.
Clarke, D. W.; Mohtadi, C.; Tuffs, P. *Automatica* **1987**, *23*, 137–148.
Boucher, P.; Dumur, D. *La commande prédictive*; Editions Technip, 1996; Vol. 8.

7. RESPONSIBILITY NOTICE

The authors are the only responsible for the printed material included in this paper.